Surface Urban Heat and Cool Islands and Their Drivers: An Observational Study in Nanjing, China

LIANG WANG,[a] DAN LI,[a] NING ZHANG,[b] JIANNING SUN,[b] AND WEIDONG GUO[b]

[a] *Department of Earth and Environment, Boston University, Boston, Massachusetts*
[b] *School of Atmospheric Sciences, Nanjing University, Nanjing, China*

(Manuscript received 7 April 2020, in final form 18 September 2020)

ABSTRACT: Urban heat islands (UHIs) are caused by a multitude of changes induced by urbanization. However, the relative importance of biophysical and atmospheric factors in controlling the UHI intensity remains elusive. In this study, we quantify the magnitude of surface UHIs (SUHIs), or surface urban cool islands (SUCIs), and elucidate their biophysical and atmospheric drivers on the basis of observational data collected from one urban site and two rural grassland sites in and near the city of Nanjing, China. Results show that during the daytime a strong SUCI effect is observed when the short grassland site is used as the reference site whereas a moderate SUHI effect is observed when the tall grassland is used as the reference site. We find that the former is mostly caused by the lower aerodynamic resistance for convective heat transfer at the urban site and the latter is primarily caused by the higher surface resistance for evapotranspiration at the urban site. At night, SUHIs are observed when either the short or the tall grassland site is used as the reference site and are predominantly caused by the stronger release of heat storage at the urban site. In general, the magnitude of SUHI is much weaker, and even becomes SUCI during daytime, with the short grassland site being the reference site because of its larger aerodynamic resistance. The study highlights that the magnitude of SUHIs and SUCIs is mostly controlled by urban–rural differences of biophysical factors, with urban–rural differences of atmospheric conditions playing a minor role.

KEYWORDS: Surface fluxes; Heat islands; Urban meteorology

1. Introduction

Urban population, which makes up more than half of the world's population, is projected to reach 68% by 2050 (United Nations 2019). A well-known consequence of urbanization is the urban heat island (UHI) effect, which describes the fact that urban areas are generally hotter than the surrounding rural areas, especially at night (Oke et al. 2017). UHIs exacerbate the heat stress for city dwellers (Mora et al. 2017; Rydin et al. 2012; Zhao et al. 2018) and threaten urban sustainability in terms of ecosystem functions, energy consumption, and air quality (Grimm et al. 2008). The UHI intensity can be quantified through the urban–rural contrast of air and/or surface temperatures. In this study, we focus on the urban–rural contrast of surface temperature T_s, herein surface urban heat islands (SUHIs). Negative urban–rural contrasts in terms of the surface temperature, which are sometimes observed, are called surface urban cool islands (SUCIs).

SUHIs, and UHIs in general, are induced by the unique characteristics of urban environments such as the larger anthropogenic emissions, the lower albedo owing to the use of certain man-made materials and radiative trapping, less evaporative cooling associated with limited green space and low surface moisture, as well as the larger heat release at night due to the higher thermal admittance of built materials (Arnfield 2003; Grimm et al. 2008; Grimmond 2007; Oke 1982; Ramamurthy et al. 2014; Taha 1997; Zhao et al. 2014). A logical starting point to understand the drivers of SUHIs is to use the surface energy balance equation. For a volume of outdoor space that extends from the infinitesimal interfacial layer below the surface to the top of buildings, the surface energy balance equation can be expressed as

$$R_n + \mathrm{AF} + \mathrm{AH} = H + \mathrm{LE} + G, \tag{1}$$

where R_n is the net radiation, AF is the anthropogenic heat release within the volume, and AH is the net horizontal heat transfer by wind. The sum of these three terms is the total energy input to the control volume, which is partitioned into the sensible heat flux H, the latent heat flux LE, and the ground heat flux or heat storage G. From Eq. (1) one can see that a larger anthropogenic heat flux or a larger net radiation (e.g., caused by a lower albedo) in the urban environment means more energy inputs, thus favoring higher SUHIs. In contrast, a larger heat flux going into the ground, which often occurs during daytime, tends to cool the surface, which may cause SUCIs. The opposite tends to occur during nighttime, which heats the surface and leads to strong SUHIs. Similarly, a larger sensible/latent heat flux going into the atmosphere would cool the surface while a larger sensible/latent heat flux from the atmosphere to the surface would heat the surface. The sensible and latent heat fluxes are turbulent fluxes that are strongly controlled by aerodynamic features and vegetation/moisture conditions at the surface. In particular, urban areas usually have limited vegetation cover and low soil moisture, which tends to cause lower latent heat fluxes into the atmosphere and thus SUHIs. One way to link the sensible and latent heat fluxes

Supplemental information related to this paper is available at the Journals Online website: https://doi.org/10.1175/JAMC-D-20-0089.s1.

Corresponding author: Dan Li, lidan@bu.edu

DOI: 10.1175/JAMC-D-20-0089.1

to surface temperature is through the concepts of aerodynamic and surface resistances (Brutsaert 2005, 1982; Monteith and Unsworth 2007), as follows:

$$H = \frac{\rho c_p}{r_a}(T_s - T_a) \quad \text{and} \tag{2}$$

$$\text{LE} = \frac{\rho L_v}{r_a + r_s}[q^*(T_s) - q_a], \tag{3}$$

where ρ is the air density, c_p is the specific heat of air at constant pressure, r_a is the aerodynamic resistance, T_a is the air temperature, L_v is the latent heat of vaporization, r_s is the surface resistance, q^* is the saturated specific humidity at T_s, and q_a is the atmospheric specific humidity. Here we use air temperature to replace potential temperature because the observational data we will be using are collected very close to the surface. It should be stressed that the aerodynamic resistance in Eq. (2) represents the efficiency with which the land convects sensible heat (i.e., not momentum) from the surface to the lower atmosphere through turbulence. While the aerodynamic resistances for both convective heat transfer and momentum transfer are affected by the mean wind shear near the surface and the gradient in the air temperature (Brutsaert 2005, 1982; Garratt 1992), there is a strong distinction between momentum and heat transfer over rough surfaces, as reviewed elsewhere (Brutsaert 1982; Li 2019) and demonstrated by recent large-eddy simulations (Li et al. 2020; Li and Bou-Zeid 2019). A rougher surface characterized by a larger momentum roughness length, which is a concept closely related to the building geometry in urban areas (Oke et al. 2017), does not necessarily imply a higher efficiency for convective heat transfer. In fact, there are ''trade-off effects'' in the effectiveness of a very-rough surface in exchanging momentum and scalars (e.g., heat) with a turbulent boundary layer (Li et al. 2020). As the surface becomes rougher in terms of momentum transfer, convective heat transfer may or may not become more efficient (Li et al. 2020), namely, the aerodynamic resistance for convective heat transfer may or may not decrease. In comparison, the surface resistance in Eq. (3) represents the efficiency with which the land extracts water from the saturated zone to the soil surface or from the vegetation inside to the leaf surface, and it is strongly dependent on soil moisture and vegetation stresses (Brutsaert 2005, 1982; Garratt 1992). The lack of vegetation and the prevalence of impervious surface in urban areas imply that the urban surface resistance is often larger than its rural counterpart.

Many studies explore the importance of each energy component in the surface energy balance equation in controlling the magnitude of SUHIs or SUCIs. Nighttime SUHIs are known to be mostly caused by the larger heat release at night due to the higher thermal admittance of built materials and the larger anthropogenic heat flux in urban areas (Oke et al. 2017). On the other hand, daytime SUHIs are thought to be primarily caused by the lack of evaporative cooling in cities, with other factors such as the urban–rural difference in albedo also playing important roles (Carlson and Boland 1978; Gu and Li 2018; Imhoff et al. 2010; Li et al. 2019; Oke 1982; Peng et al. 2012; Taha 1997; Zhou et al. 2016). However, there is a recent debate regarding the dominant factor controlling the spatial variations of daytime SUHIs within the context of large-scale urban modeling. The study by Zhao et al. (2014) found that the spatial variations of the daytime SUHIs in North America can be largely explained by the spatial variations of the urban–rural difference in the aerodynamic resistance, which seems to be at odds with the traditional paradigm that attributes the daytime SUHIs mainly to the lack of evaporative cooling in cities. According to their analysis (Zhao et al. 2014), stronger SUHIs in wetter climates are caused by the fact that the rural areas have higher efficiencies to transfer sensible heat from the surface into the lower atmosphere than the urban areas; while weaker SUHIs or even SUCIs in drier climates are due to that the rural areas have lower convective heat transfer efficiencies than the urban areas. Later, Li et al. (2019) argued that the spatial variations of daytime SUHIs over North America are more controlled by the spatial variations of urban–rural difference in the surface resistance, with the spatial variations of urban–rural difference in the aerodynamic resistance also playing a role (see also Manoli et al. 2019). In a wetter climate, the rural vegetation tends to have a higher evaporative cooling capacity and thus the SUHI is stronger.

Both studies by Zhao et al. (2014) and Li et al. (2019) used subgrid outputs from offline land simulations with global climate or Earth system models (Li et al. 2016a,b; Oleson et al. 2008b,a) to diagnose the spatial variations of SUHIs at continental scales. The use of subgrid outputs from global climate or Earth system models allows (or equivalently forces) them to assume that urban and rural lands share the same atmospheric conditions, so the urban–rural difference in surface temperature is solely a result of urban–rural differences in surface biophysical factors. The objective of this study is to revisit this debate using observational data collected at paired flux tower sites across urban–rural gradients and to assess the assumption of similar atmospheric conditions between urban and rural land made by Zhao et al. (2014) and Li et al. (2019) as well as other studies using global climate or Earth system model outputs.

To do so, we need to extend the framework used in Zhao et al. (2014) and Li et al. (2019), which largely follows Lee et al. (2011), to consider urban–rural differences in atmospheric conditions that do exist in the real world. This is motivated by previous attempts trying to apply the framework used in Zhao et al. (2014) and Li et al. (2019) to diagnosing surface temperature differences measured by paired flux towers but those attempts either ignored the atmospheric differences (Burakowski et al. 2018), or only considered the near-surface air temperature difference but ignored other key parameters such as incoming shortwave radiation (Chen and Dirmeyer 2016; Liao et al. 2018; Wang et al. 2017). In this study, we will conduct a more comprehensive attribution of SUHIs (or SUCIs), with the aim of more appropriately quantifying the contributions from urban–rural differences in atmospheric factors, in addition to those from surface biophysical factors, to the SUHIs (or SUCIs).

The paper is organized as follows: section 2 describes the data and method, section 3 presents the main results,

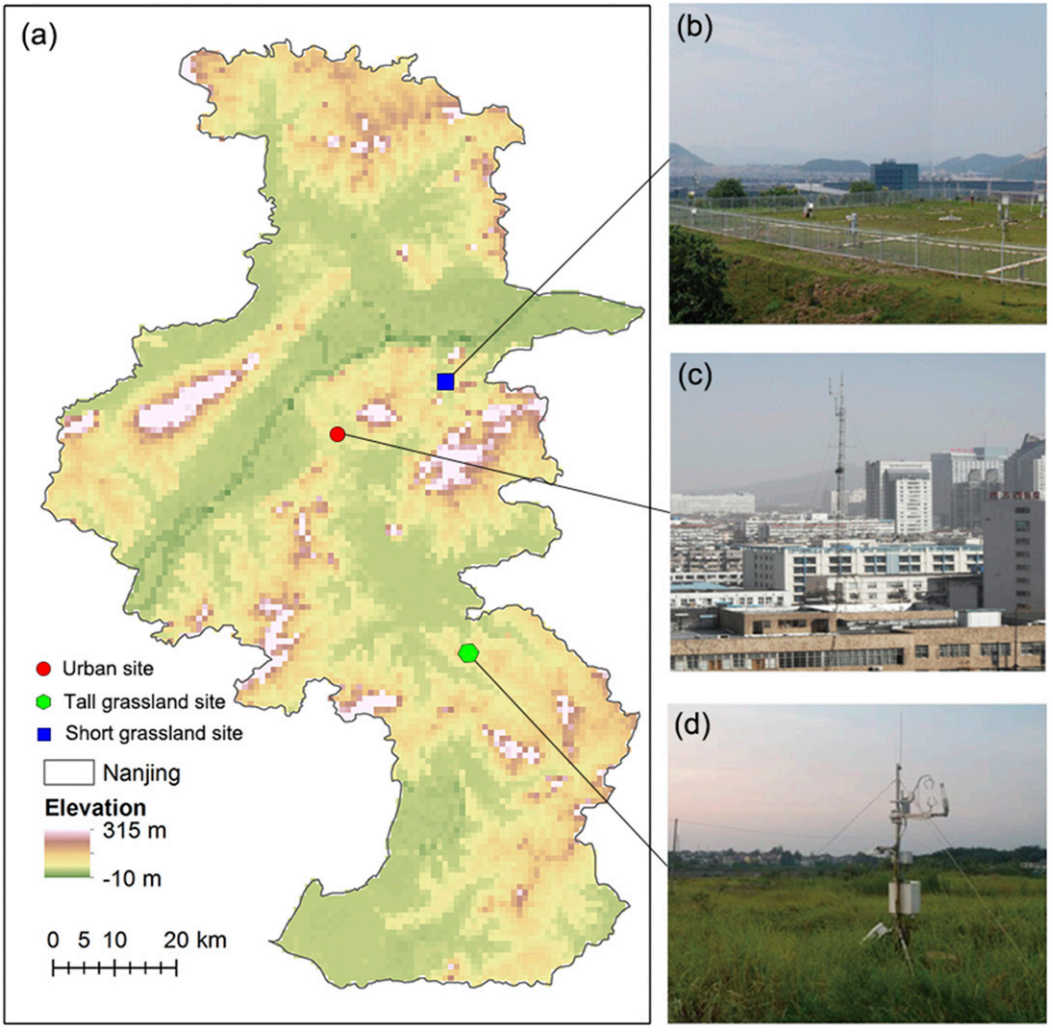

FIG. 1. (a) Locations, elevations, and land-use types of (b) the short grassland site, (c) the urban site, and (d) the tall grassland site.

and section 4 concludes the paper and discusses the implications and future work.

2. Data and method

a. Observational data

The observational data used in this study are collected at one urban site and two rural (grassland) sites in Nanjing, China (Fig. 1). We use two rural reference sites since it allows for an exploration of the influence of the selection of reference site on the computed SUHIs and the associated drivers. The urban site (32°2′24″N, 118°47′24″E) is located in the central area of Nanjing and surrounded by residential and commercial buildings with an average building height of 19.7 m and building coverage up to 70%. One of the rural sites (32°7′14″N, 118°57′10″E) is located in the Xianlin Campus of Nanjing University in eastern suburb of Nanjing. This rural site is located over short grassland with an average height of 7 cm and is 18 km away from the urban site. Another rural site (31°43′08″N, 118°58′51″E) is located in the Lishui County of Nanjing, which is 38 km away from the urban site. The land-cover type is also grassland, but the grass height is much taller with an average value of 60 cm. Therefore, we refer to this rural site as the tall grassland site and the previously mentioned rural site as the short grassland site. Automatic weather stations (Campbell Scientific model AG1000) are employed to measure air temperature, humidity and wind speed at 2 m, air pressure at 8 m, and radiation fluxes at 1.5 m. Turbulent heat fluxes are measured by the eddy covariance system (Campbell Scientific EC3000) deployed at 3 m at the two grassland sites and 36.5 m above a 22-m-high building at the urban site. All of the turbulent flux measurements are strictly screened and quality controlled following Guo et al. (2016) and Wang et al. (2017). The data used in this study are measurements at half-hourly intervals during the two summers (June, July, and August) in 2012 and 2013. This period is chosen because the measurements are relatively complete.

More detailed descriptions of the sites and instruments can be found in Guo et al. (2016) and Wang et al. (2017).

b. The attribution method

In this study, we use the two-resistance mechanism (TRM) model (Chen et al. 2020; Li et al. 2019; Li and Wang 2019; Liao et al. 2018; Moon et al. 2020; Rigden and Li 2017; Wang et al. 2019) to attribute the SUHI or SUCI to contributions from different surface and atmospheric factors. The TRM model starts from the surface energy balance equation given by

$$R_n = \mathrm{SW_{in}}(1-\alpha) + \varepsilon \mathrm{LW_{in}} - \varepsilon\sigma T_s^4 = H + \mathrm{LE} + G, \quad (4)$$

where R_n is again the net surface radiation, $\mathrm{SW_{in}}$ is the incoming shortwave radiation, α is the surface albedo, ε is the surface emissivity, $\mathrm{LW_{in}}$ is the incoming longwave radiation, σ is the Stephan–Boltzmann constant, T_s is the surface temperature, H is the sensible heat flux, LE is the latent heat flux, and G is the ground heat flux. Comparing Eq. (1) and Eq. (4) indicates that the effects of anthropogenic heat flux and the net horizontal heat transfer by wind are implicitly lumped into G when G is estimated as the residual in Eq. (4).

Substituting Eqs. (2) and (3) into Eq. (4) yields a nonlinear equation for T_s, which is further linearized by applying first-order Taylor series expansion to the outgoing longwave radiation and the saturated specific humidity terms, so that an analytical expression for T_s can be obtained:

$$T_s = \frac{\mathrm{SW_{in}}(1-\alpha) + \varepsilon \mathrm{LW_{in}} - \varepsilon\sigma T_a^4 - G - \dfrac{\rho L_v}{r_a + r_s}[q^*(T_a) - q_a]}{4\varepsilon\sigma T_a^3 + \dfrac{\rho c_p}{r_a} + \dfrac{\rho L_v}{(r_a + r_s)}\left.\dfrac{\partial q^*}{\partial T}\right|_{T_a}} + T_a. \quad (5)$$

Further, the difference in the surface temperature between urban and rural sites is expressed as the sum of the contributions from various factors using first-order Taylor series expansion of Eq. (5), as follows:

$$\begin{aligned}\Delta T_s = {} & \left(\frac{\partial T_s}{\partial \varepsilon}\right)\Delta\varepsilon + \left(\frac{\partial T_s}{\partial \alpha}\right)\Delta\alpha + \left(\frac{\partial T_s}{\partial G}\right)\Delta G + \left(\frac{\partial T_s}{\partial r_a}\right)\Delta r_a \\ & + \left(\frac{\partial T_s}{\partial r_s}\right)\Delta r_s + \left(\frac{\partial T_s}{\partial \mathrm{SW_{in}}}\right)\Delta\mathrm{SW_{in}} + \left(\frac{\partial T_s}{\partial \mathrm{LW}_{in}}\right)\Delta\mathrm{LW_{in}} \\ & + \left(\frac{\partial T_s}{\partial T_a}\right)\Delta T_a + \left(\frac{\partial T_s}{\partial q_a}\right)\Delta q_a + \left(\frac{\partial T_s}{\partial P}\right)\Delta P, \end{aligned} \quad (6)$$

where P is the near-surface air pressure and Δ indicates the urban–rural difference in each factor (i.e., urban minus rural values). The partial derivative represents the sensitivity of the surface temperature to the change in each factor, whose analytical formulation can be directly obtained using Eq. (5). Throughout the paper, each term on the right-hand side of Eq. (6) will be called a "contribution." Each contribution is composed of two parts: the sensitivity (Table 2) and the difference (Table 3). The sensitivity refers to how strongly the surface temperature responds to a change in each factor. The difference refers to the change in each factor when comparing the urban and rural sites (i.e., urban minus rural values). As compared with previous studies using the TRM method (Li et al. 2019; Li and Wang 2019; Liao et al. 2018; Rigden and Li 2017), this equation considers the factors affecting SUHIs more comprehensively.

To facilitate our discussion, we categorize the variables and parameters on the rhs of Eq. (6) into two groups: surface biophysical factors and atmospheric factors. Surface biophysical factors include emissivity, albedo, ground heat flux, aerodynamic resistance, and surface resistance, which are strong functions of land-use type. Atmospheric factors include incoming shortwave radiation, incoming longwave radiation, air temperature, air specific humidity, and air pressure, which are primarily determined by local background climate and weather conditions. We note that aerodynamic resistance and surface resistance in theory depend on both surface biophysical and atmospheric conditions (Brutsaert 2005, 1982; Monteith and Unsworth 2007), but here they are treated as surface biophysical factors for simplicity. These surface and atmospheric factors, together with surface temperature, fully describe the TRM model.

c. Application of the attribution method to the observational data

Most of the required inputs of the TRM model can be obtained directly from the observations. We assume constant emissivity values of 0.95, 0.93, and 0.97 for the urban, short grassland and tall grassland sites, respectively (Oke et al. 2017). Sensitivity tests on these emissivity values are conducted, and the results are presented in the online supplemental material. Based on these prescribed emissivity values, the surface temperature is estimated from the measurements of the outgoing longwave radiation (after subtracting the reflected longwave radiation). Again, the ground heat flux is estimated as the residual of the surface energy balance equation and thus implicitly includes the effects of anthropogenic heat flux, advective flux, as well as measurement errors. The well-known surface energy imbalance is also lumped into the ground heat flux (Foken 2008; Franssen et al. 2010; Leuning et al. 2012; Liu et al. 2011; Mauder et al. 2013; Stoy et al. 2013). The air specific humidity is calculated from the observed vapor pressure and the near-surface air pressure. Then the aerodynamic and surface resistances can be inferred using Eqs. (2) and (3), respectively. These calculations are all conducted at the half-hourly scale.

The performance of the TRM model can be evaluated by the extent to which the modeled ΔT_s and the observed ΔT_s are consistent with each other. Acceptable agreement between the TRM-modeled ΔT_s and that inverted from the observed outgoing longwave radiation is the prerequisite for the model to correctly attribute the SUHI. Therefore, in order to improve the model performance, three strategies are adopted following Liao et al. (2018).

First, we find that by aggregating the input variables to the daily scale first and then performing the attribution, the accuracy of the TRM model is higher than that by conducting the attribution at the half-hourly scale and then aggregating the results to the daily scale, which confirms the finding by Liao et al. (2018). Therefore, in this paper, we apply the TRM model to the daytime and nighttime averaged data separately.

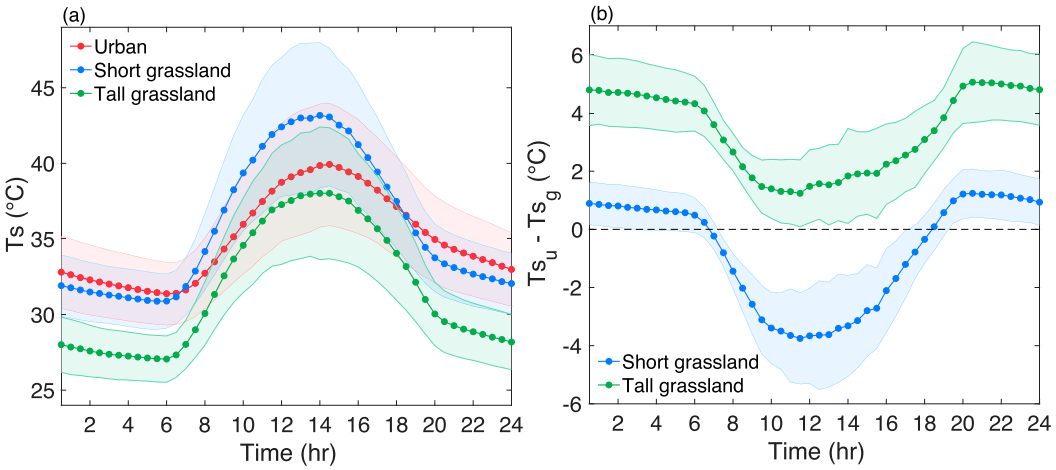

FIG. 2. Average diurnal cycles of (a) surface temperatures and (b) differences in surface temperature between the urban site and the grassland sites (urban minus grassland). The shading denotes standard deviations.

We define daytime (1000–1600) and nighttime (2200–0400) on the basis of the local time.

Second, before aggregating the data to the daily scale, we apply several data-filtering criteria to the original data at the half-hourly scale. The basic data-filtering strategy is to exclude the half-hourly data when any one of the three sites has a missing value, since only by doing so can the data from different sites be compared. The more stringent data-filtering strategy only employed by the TRM model is to exclude the data where the absolute value of the sensible heat flux or latent heat flux is small (less than $15\,\mathrm{W\,m^{-2}}$ for daytime and $0.1\,\mathrm{W\,m^{-2}}$ for nighttime) and where the inferred aerodynamic resistance or surface resistance is negative. As shall be seen later, the more stringent data filtering does not change ΔT_s much and its main effect is to reduce the uncertainties, especially at night.

Third, we adopt the weighted average approach (Liao et al. 2018) to calculate the partial derivatives (e.g.,$\partial T_s/\partial\alpha$) in the model, as follows:

$$X = \frac{X_{\mathrm{urban}} + mX_{\mathrm{rural}}}{1+m}, \tag{7}$$

where X is the final partial derivative used in the model, m is average weight, and X_{urban} and X_{rural} are the partial derivatives calculated only using data from the urban site and the rural site, respectively. The introduction of m is to account for the effects of neglected higher-order and cross-order terms in the Taylor series expansion, which can be important when the urban–rural differences are not small. We optimize the value of m by minimizing the root-mean-square error between the modeled and observed ΔT_s (Liao et al. 2018).

3. Results

In the following, we first examine the urban–rural differences in surface temperature and various factors using average diurnal cycles. We then quantitatively attribute the observed SUHIs or SUCIs to each factor based on the TRM model.

a. *Observed urban–rural differences in surface temperature and fluxes*

This section presents the urban–rural differences in surface temperature and fluxes based upon average diurnal cycles over the two summers (June, July, and August) in 2012 and 2013. During the daytime (1000–1600, local standard time), the urban site is on average 3.3°C cooler than the short grassland site, showing a strong SUCI, but 1.6°C hotter than the tall grassland site, showing a moderate SUHI (Fig. 2). At night (2200–0400, local standard time), it shows a very strong SUHI (4.8°C on average) when the tall grassland site is used as the reference site while only a weak SUHI (0.9°C on average) when the short grassland site is used as the reference site. The observed urban–rural differences in surface temperature are closely related to the urban–rural differences in the fluxes involved in Eq. (1), as discussed below.

First, we examine the incoming radiative fluxes that are important atmospheric factors affecting surface temperature. During the daytime, the incoming shortwave radiation $\mathrm{SW_{in}}$ of the urban site is on average lower than that of the two grassland sites (Fig. 3a), which may be associated with air pollution (Estournel et al. 1983; Gan et al. 2014; Jáuregui and Luyando 1999; Peterson and Flowers 1977) and cloud cover (Stanhill and Moreshet 1994; Wang et al. 2015). Hence the urban–rural differences in the incoming shortwave radiation do not fully explain the urban–rural differences in surface temperature as they would always lead to SUCIs. However, the incoming longwave radiation $\mathrm{LW_{in}}$ seems to play an important role in nighttime SUHIs since $\mathrm{LW_{in}}$ at the urban site is on average larger than that of the short grassland site by $5.8\,\mathrm{W\,m^{-2}}$ and larger than that of the tall grassland site by $6.7\,\mathrm{W\,m^{-2}}$ at night (Fig. 3b). This is consistent with the higher urban air temperature at night (Fig. 4c). We acknowledge that the incoming longwave radiation is affected by other factors such as the emissivity of air, which further depends on the amounts of water vapor and aerosols (Brutsaert 2005), but previous studies seem to show that their impacts on the urban–rural contrast of incoming longwave radiation are small (Aida and Yaji 1979;

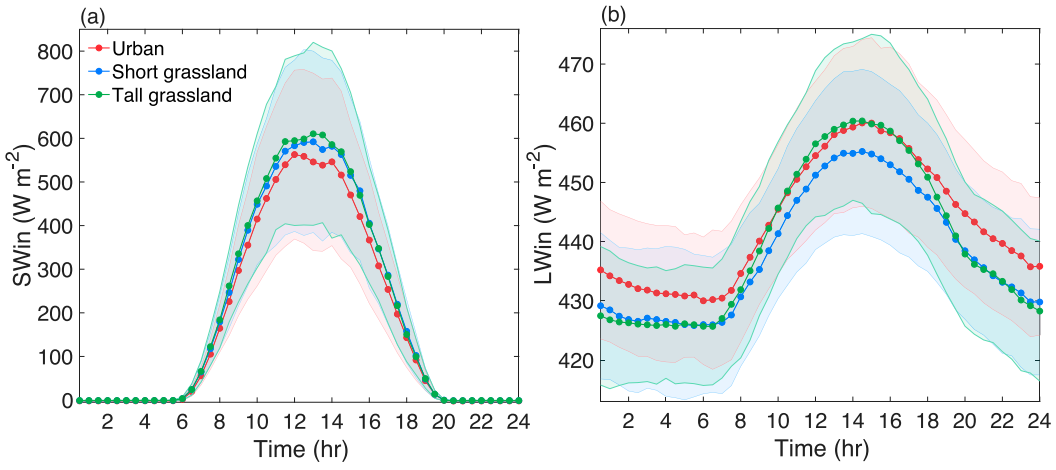

FIG. 3. Average diurnal cycles of incoming (a) shortwave and (b) longwave radiation fluxes. The shading denotes standard deviations.

Ao et al. 2019; Estournel et al. 1983; Li et al. 2015; Núñez et al. 2000; Oke and Fuggle 1972).

Second, we seek to attribute the unexplained portion to the turbulent fluxes. During the daytime, the sensible heat flux H of the urban site is 56 W m^{-2} larger than that of the short grassland site (Fig. 4a), which also leads to the SUCI effect as SW_{in}. This is related to two factors. First, the overlying air over the urban surface is 0.4°C cooler than that over the short grassland (Fig. 4c), which creates a larger land–atmosphere temperature gradient and thus creates a larger sensible heat flux at the urban site. Second, with a certain land–atmosphere temperature gradient, the sensible heat flux is directly determined by the efficiency with which the land surface convects heat into the overlying atmosphere, which is higher at the urban site reflected by the lower aerodynamic resistance r_a by 117.0 s m^{-1} (Fig. 4e). In contrast, the urban aerodynamic resistance is higher than that of the tall grassland site by 28.3 s m^{-1}, and therefore the sensible heat flux of the urban site is only on average 2.6 W m^{-2} higher than that of the tall grassland site. We also notice there are slight shifts in the peak time of sensible heat flux between urban and grassland sites, which is mainly due to the high thermal admittance of built materials in urban areas and the radiative trapping in the urban canyon (Oke et al. 2017; Ramamurthy et al. 2014). At night, the sensible heat fluxes of the grassland sites become negative, implying that the atmosphere in turn heats the grassland surfaces. But the urban surface still heats the atmosphere with a positive sensible heat flux, which was also observed by many previous studies (Grimmond and Oke 1995; Grimmond et al. 2004; Kalanda et al. 1980; Offerle et al. 2006; Oke 1988; Yap and Oke 1974).

As for the latent heat flux, during the daytime, the urban site has a much lower latent heat flux than that of the rural sites (Fig. 4b). According to Eq. (3), it is the larger surface resistance of the urban site, which is 562.1 and 615.9 s m^{-1} larger than those at the short and tall grassland sites, respectively (Fig. 4f), that leads to the smaller latent heat flux of the urban site and the daytime SUHI. The small latent heat flux of the urban site is mainly due to the lower vegetation fraction (i.e., higher impervious surface fraction; see Fig. 1), lower moisture availability caused by faster runoff over impervious surfaces, as well as negligible irrigation at this urban site. The smaller latent heat flux of urban surfaces has been widely observed before (Christen and Vogt 2004; Cleugh and Oke 1986; Grimmond et al. 2004; Kalanda et al. 1980). In contrast, at night, the latent heat flux at the urban site is on average slightly larger than that at the two grassland sites mainly because of the drier air over the urban surface (Fig. 4d).

Last, we examine the ground heat flux G. Because of the higher thermal admittance of the built material in urban areas, the urban surface tends to store more heat into the ground during daytime and release more heat to heat the surface at night (Oke et al. 2017). Therefore, the ground heat flux of the urban site is on average higher than that of the two grassland sites (Fig. 5). At night, the absolute magnitude of ground heat flux at the urban site remains higher, indicating stronger heat release from the urban ground and contributes to SUHIs.

b. *Attribution results*

Before we discuss the attribution results, we first evaluate the SUHIs or SUCIs estimated by the TRM model. We find good agreement between the observed and the modeled urban–rural differences in the surface temperature, as illustrated by the dark red and dark green bars in Fig. 6. Similar to what we found in section 3a, we identify a strong daytime SUCI and a weak nighttime SUHI when using the short grassland site as a reference, while a moderate daytime SUHI and a strong nighttime SUHI when using the tall grassland site as a reference. We highlight that this is not a validation for the modeled T_s but rather the modeled ΔT_s. This validation remains important because even a model that captures T_s does not necessarily capture ΔT_s due to the linearization process involved in the first-order Taylor series expansion [Eq. (6)]. This has been demonstrated by a recent paper by Liao et al. (2018), who argued that acceptable agreement between observed and modeled ΔT_s is the prerequisite for the model to correctly attribute ΔT_s.

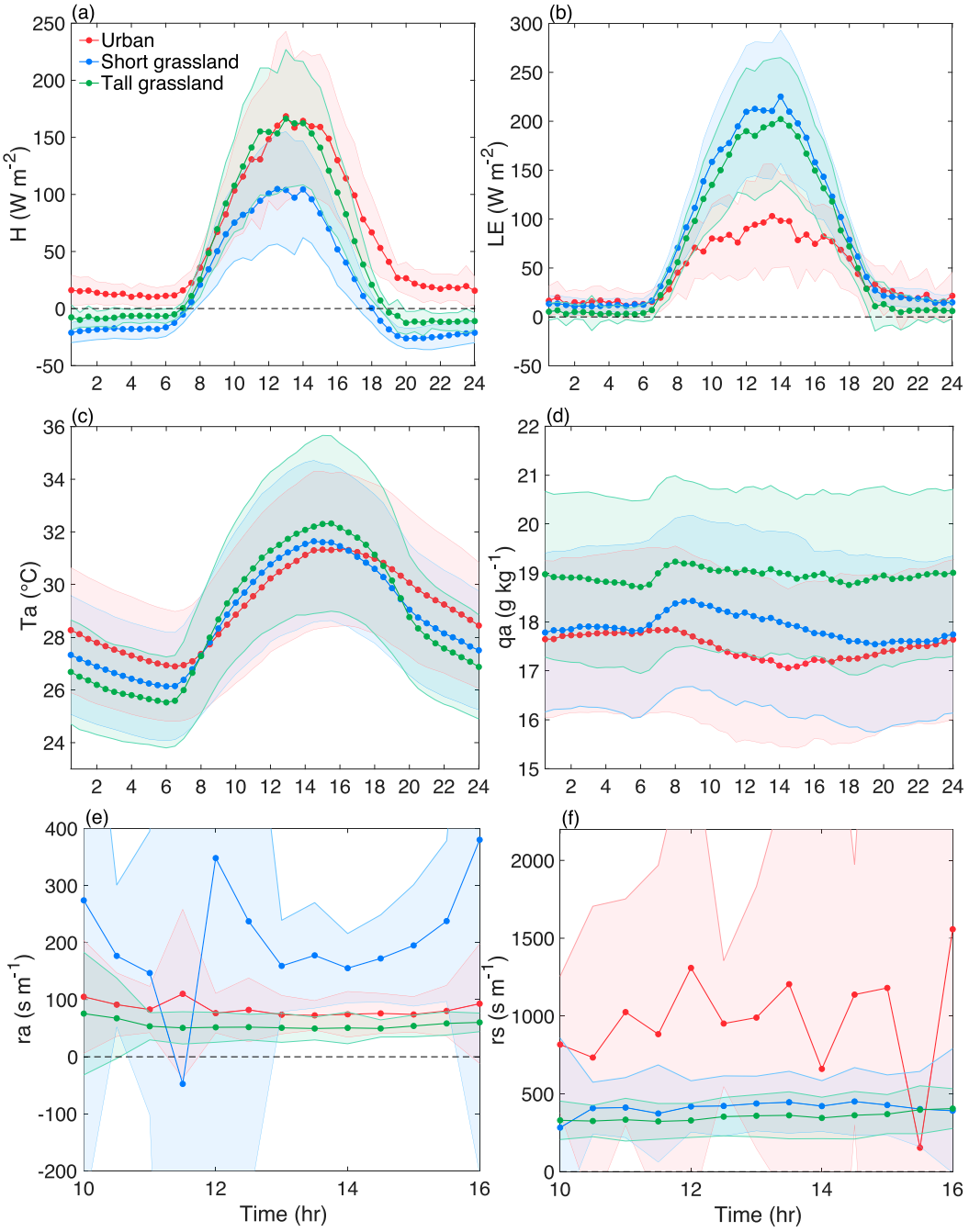

FIG. 4. Average diurnal cycles of (a) sensible and (b) latent heat fluxes and their controlling factors, including (c) air temperature, (d) air specific humidity, (e) aerodynamic resistance, and (f) surface resistance. For (e) and (f), only the daytime (1000–1600 LT) results are shown. The shading denotes standard deviations.

We also evaluate the effect of the stringent data filtering used by the TRM model (cf. the light and dark red/green bars in Fig. 6). One can see reasonable consistency in ΔT_s no matter whether the stringent data filtering discussed in section 2c is used. Therefore, the stringent data filtering does not change ΔT_s much and its main effect is to reduce the uncertainties (represented by the error bars), especially at night. Below we focus on discussing individual contributions when the stringent data filtering is applied (the dark-blue bars in Fig. 6 and also the values presented in Tables 1 to 3).

1) DAYTIME ATTRIBUTION RESULTS

During the daytime and when the short grassland site is used as the reference site, the aerodynamic resistance, ground heat

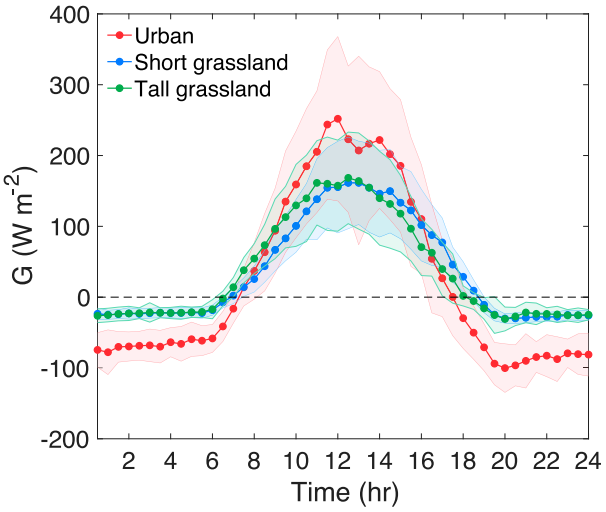

FIG. 5. Average diurnal cycle of ground heat flux. The shading denotes standard deviations.

flux, and incoming shortwave radiation contribute −167%, −87%, and −53%, respectively, to the urban–rural surface temperature difference, which are offset by the positive contributions from the surface resistance (183%) and albedo (30%) (see Fig. 6a and Table 1). The other factors make much smaller contributions than these five factors. Therefore, the largest contributions come from the aerodynamic resistance (negative) and the surface resistance (positive). The negative contribution from aerodynamic resistance is related to the fact that the urban site has a lower aerodynamic resistance for convective heat transfer than the short grassland site (Fig. 4e), which contributes to higher sensible and latent heat fluxes and thus a cooler surface. The sensitivity of surface temperature to the aerodynamic resistance is positive and about $7 \times 10^{-2}\,\mathrm{K\,m\,s^{-1}}$ (Table 2), implying that the surface temperature tends to increase when the surface becomes smoother. The urban–rural difference in terms of aerodynamic resistance is $-8 \times 10\,\mathrm{s\,m^{-1}}$ (Table 3), which, combined with the positive sensitivity, leads to a large negative contribution. In contrast, the urban site has a higher surface resistance than the short grassland site (Fig. 4f), which contributes to a lower latent heat flux and thus a hotter surface. The sensitivity of surface temperature to the surface resistance is positive and about $9 \times 10^{-3}\,\mathrm{K\,m\,s^{-1}}$, implying that the surface temperature tends to increase when the surface becomes drier. The urban–rural difference in terms of surface resistance is also positive ($6 \times 10^{2}\,\mathrm{s\,m^{-1}}$), which leads to a large positive contribution. We note that although their contributions are close in terms of magnitude, the underlying mechanisms are different: the surface

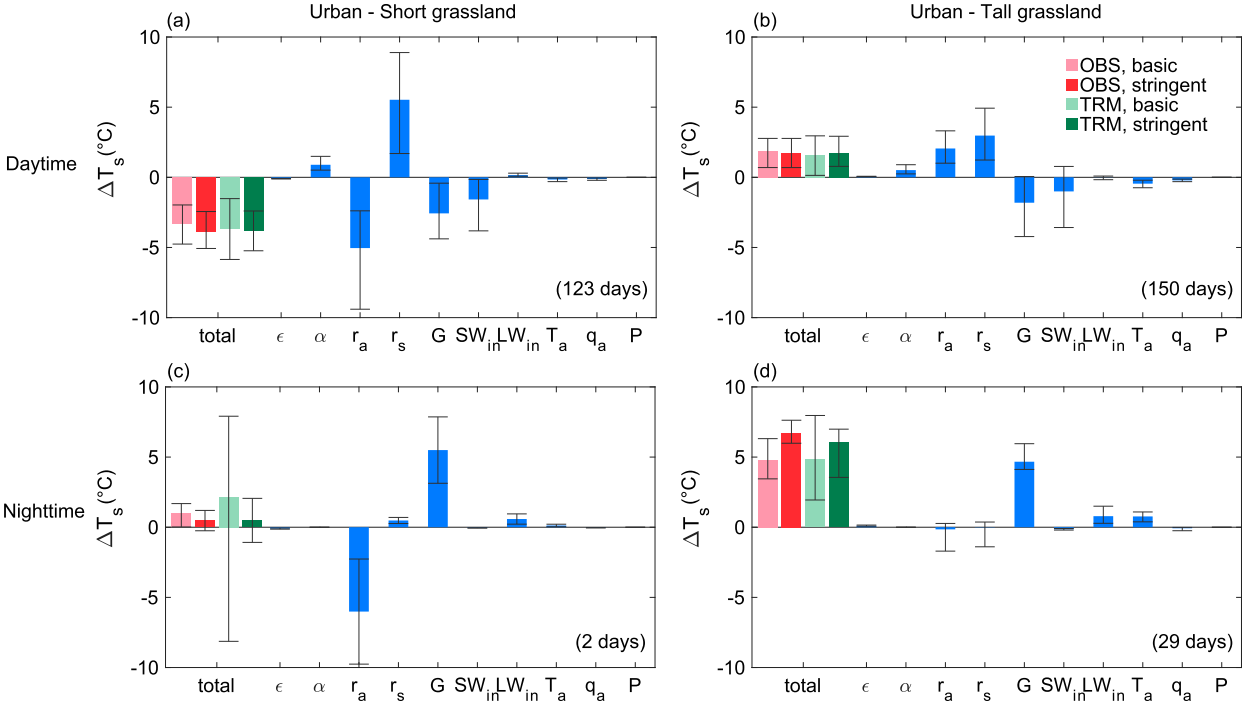

FIG. 6. Attribution results of surface urban heat islands using the TRM model during (a), (b) daytime (1000–1600) and (c), (d) nighttime (2200–0400), using (left) the short grassland site and (right) the tall grassland site as the reference site. The sample size is noted in parentheses in the bottom-right corner of each panel. The column indicates the median of the results at the daily scale, and the upper and lower error bars are the 80th and 20th percentiles of the results, respectively, representing the day-to-day variability of the attribution results. "Basic" refers to applying the basic data-filtering strategy, in which we only exclude the half-hourly data when any one of the three sites has a missing value. "Stringent" refers to applying the more stringent data-filtering strategy, in which we further exclude the data when absolute value of the sensible heat flux or latent heat flux is small (less than 15 W m^{-2} for daytime and 0.1 W m^{-2} for nighttime) and when the inferred aerodynamic resistance or surface resistance is negative.

TABLE 1. The surface urban heat islands and the attribution results (°C). In all tables, DS = daytime with the short grassland site as the reference site, DT = daytime with the tall grassland site as the reference site, NS = nighttime with the short grassland site as the reference site, and NT = nighttime with the tall grassland site as the reference site. The value is the median of the results at the daily scale. As a result, the values reported here will not be equal to the products of the values reported in Table 2 and those in Table 3.

	Sum	ε	α	r_a	r_s	G	SW_{in}	LW_{in}	T_a	q_a	P
DS	−3.0	−0.1	0.9	−5.0	5.5	−2.6	−1.6	0.2	−0.2	−0.1	0.0
DT	2.2	0.1	0.5	2.1	3.0	−1.8	−1.0	0.0	−0.5	−0.2	0.0
NS	0.5	−0.1	0.0	−6.0	0.5	5.5	−0.1	0.6	0.1	0.0	0.0
NT	6.0	0.1	0.0	−0.2	0.0	4.7	−0.1	0.8	0.8	−0.1	0.0

temperature is an order of magnitude more sensitive to aerodynamic resistance than to surface resistance, but the urban–rural difference in terms of aerodynamic resistance is an order of magnitude smaller than its surface resistance counterpart.

Moreover, the urban site has a larger ground heat flux than the short grassland site (Fig. 5), which helps build a cooler surface by conducting more heat from the surface into the ground during the daytime. The sensitivity of surface temperature to ground heat flux is negative (Table 2), and the urban–rural difference of ground heat flux is positive (Table 3), which leads to a moderate negative contribution. In contrast, the urban site has a lower incoming shortwave radiation than the short grassland site (Fig. 3a), which contributes to a lower surface temperature. Here, the sensitivity of surface temperature to the incoming shortwave radiation is positive, while the urban–rural difference of incoming shortwave radiation is negative, resulting in a small negative contribution. When compared with the contribution made by the ground heat flux, the contribution from the incoming shortwave radiation is smaller in magnitude because of the smaller urban–rural difference in terms of incoming shortwave radiation (Table 3). In addition, the urban site has a lower albedo than the short grassland site, which favors more energy inputs and thus a hotter surface. The sensitivity and urban–rural difference for the albedo are both negative, leading to a small positive contribution (Tables 2 and 3).

In summary, the cooler urban surface during daytime, when compared with the short grassland surface, is mainly caused by its higher efficiency in convective heat transfer and the larger heat storage. The larger surface resistance over the urban surface tends to make it hotter but does not overcome the negative contributions from aerodynamic resistance and ground heat flux. The most important atmospheric variable that needs to be considered in the attribution is the incoming shortwave radiation, whose difference between urban and rural sites plays a minor but nonnegligible role.

During the daytime but when the tall grassland site is used as the reference site, the surface resistance, aerodynamic resistance, and albedo make positive contributions of 136%, 95%, and 24%, respectively (Fig. 6b and Table 1). The ground heat flux, incoming shortwave radiation, and air temperature make negative contributions of 82%, 45%, and 23%, respectively. The strongest positive contribution from surface resistance is related to the fact that the urban site has a larger surface resistance than the tall grassland site (Fig. 4f), which favors a lower latent heat flux and thus a hotter surface. The sensitivity of surface temperature to surface resistance is positive (Table 2), and the urban–rural difference of surface resistance is also positive (Table 3), which leads to a large positive contribution. The urban site also has a larger aerodynamic resistance than the tall grassland site (Fig. 4e), which contributes to lower turbulent heat fluxes and thus a hotter surface. Here the sensitivity of surface temperature to aerodynamic resistance is positive ($8 \times 10^{-2}\,K\,m\,s^{-1}$), and the urban–rural difference of aerodynamic resistance is also positive ($3 \times 10\,s\,m^{-1}$), which leads to a moderate positive contribution. When compared with the contribution made by the surface resistance, the aerodynamic resistance contribution is smaller mainly because of the much smaller urban–rural difference of aerodynamic resistance than that of surface resistance. In addition, the albedo of the urban site is lower than that of the tall grassland site, which contributes to its higher net radiation and thus a hotter urban surface. The sensitivity and difference for the albedo are both negative (Tables 2 and 3), leading to a minor positive contribution.

As for the negative contributions, first, the ground heat flux of the urban site is larger than that of the tall grassland site (Fig. 5), favoring a cooler surface. The sensitivity for the ground heat flux is negative and about $-4 \times 10^{-2}\,K\,m^2\,W^{-1}$, while the difference is positive and about $5 \times 10\,W\,m^{-2}$, which results in a moderate negative contribution. Second, the urban site is lower than the tall grassland site in terms of the incoming shortwave radiation (Fig. 3a), which favors a cooler urban surface. The sensitivity of surface temperature to the incoming

TABLE 2. Sensitivities of surface temperature to changes in various factors.

	$\partial T_s/\partial\varepsilon$ (K)	$\partial T_s/\partial\alpha$ (K)	$\partial T_s/\partial r_a$ ($K\,m\,s^{-1}$)	$\partial T_s/\partial r_s$ ($K\,m\,s^{-1}$)	$\partial T_s/\partial G$ ($K\,m^2\,W^{-1}$)	$\partial T_s/\partial SW_{in}$ ($K\,m^2\,W^{-1}$)	$\partial T_s/\partial LW_{in}$ ($K\,m^2\,W^{-1}$)	$\partial T_s/\partial T_a$ (—)	$\partial T_s/\partial q_a$ (K)	$\partial T_s/\partial P$ ($K\,Pa^{-1}$)
DS	-5×10^{0}	-3×10^{1}	7×10^{-2}	9×10^{-3}	-4×10^{-2}	4×10^{-2}	4×10^{-2}	3×10^{-1}	2×10^{2}	-2×10^{-5}
DT	-3×10^{0}	-2×10^{1}	8×10^{-2}	5×10^{-3}	-4×10^{-2}	3×10^{-2}	3×10^{-2}	5×10^{-1}	1×10^{2}	-3×10^{-5}
NS	-5×10^{0}	1×10^{-1}	2×10^{-3}	2×10^{-4}	-1×10^{-1}	1×10^{-1}	1×10^{-1}	1×10^{-1}	1×10^{2}	1×10^{-5}
NT	-5×10^{0}	2×10^{-1}	-1×10^{-4}	8×10^{-5}	-1×10^{-1}	8×10^{-2}	9×10^{-2}	3×10^{-1}	7×10^{1}	1×10^{-5}

TABLE 3. Urban–rural differences in terms of various factors that affect the surface temperature. (Δ: urban minus rural values).

	$\Delta\varepsilon$ (—)	$\Delta\alpha$ (—)	Δr_a ($s\,m^{-1}$)	Δr_s ($s\,m^{-1}$)	ΔG ($W\,m^{-2}$)	ΔSW_{in} ($W\,m^{-2}$)	ΔLW_{in} ($W\,m^{-2}$)	ΔT_a (K)	Δq_a (—)	ΔP (Pa)
DS	2×10^{-2}	-4×10^{-2}	-8×10^{1}	6×10^{2}	6×10^{1}	-4×10^{1}	5×10^{0}	-6×10^{-1}	-7×10^{-4}	-5×10^{1}
DT	-2×10^{-2}	-3×10^{-2}	3×10^{1}	6×10^{2}	5×10^{1}	-3×10^{1}	-3×10^{-1}	-9×10^{-1}	-2×10^{-3}	-2×10^{2}
NS	2×10^{-2}	0	-4×10^{3}	3×10^{3}	-5×10^{1}	-5×10^{-1}	5×10^{0}	9×10^{-1}	-4×10^{-4}	-7×10^{1}
NT	-2×10^{-2}	0	3×10^{2}	-2×10^{3}	-5×10^{1}	-2×10^{0}	1×10^{1}	3×10^{0}	-1×10^{-3}	-2×10^{2}

shortwave radiation is positive and about $3\times10^{-2}\,K\,m^2\,W^{-1}$, while the difference is negative and about $-3\times10\,W\,m^{-2}$, which leads to a small negative contribution. Third, the air temperature of the urban site is lower than that of the tall grassland (Fig. 4c), which contributes to a higher sensible heat flux and thus a lower surface temperature. The sensitivity of surface temperature to the air temperature is positive and about 5×10^{-1} while the difference is negative as -9×10^{-1} K, which results in a minor negative contribution.

In summary, the hotter urban surface during daytime, when compared to the tall grassland surface, is mainly because that the urban surface is drier and has a lower efficiency for convective heat transfer. While the larger heat storage tends to reduce the surface temperature, it does not overcome the effects of surface and aerodynamic resistances. The urban–rural differences in terms of atmospheric conditions, most notably incoming shortwave radiation and air temperature, play a minor but nonnegligible role.

2) NIGHTTIME ATTRIBUTION RESULTS

During the nighttime and when the short grassland site is used as the reference site, the ground heat flux makes the largest positive contribution (Fig. 6c and Table 1). At night, the ground heat flux becomes negative, which indicates that the heat stored in the ground during daytime is released to heat the surface. The urban site has a larger ground heat flux magnitude than the short grassland site, contributing to a hotter surface. The sensitivity for the ground heat flux is negative (Table 2), and the difference is also negative and large in terms of magnitude (Table 3), which leads to a very large positive contribution. The surface resistance, incoming longwave radiation, and air temperature also make slightly positive contributions. This implies that the urban surface remains drier and the urban air remains hotter at night. The positive contributions are largely offset by the negative contribution from the aerodynamic resistance.

When the tall grassland site is used as the reference site, the biggest positive contributor is still the ground heat flux (78%), followed by the incoming longwave radiation (13%) and the air temperature (13%) (Fig. 6d and Table 1). This again implies that the urban surface is hotter because of heat storage release and the urban air remains hotter. Contributions from other factors are minor.

In summary, the hotter urban surface during nighttime, when compared to either the tall grassland surface or the short grassland surface, is mainly because of the larger heat storage release. When the short grassland site is used as the reference site, the SUHI magnitude is smaller because of the stronger negative contribution from aerodynamic resistance. The urban–rural differences in terms of atmospheric conditions, most notably incoming longwave radiation and air temperature, play a minor role.

3) DIFFERENCES IN THE ATTRIBUTION RESULTS WITH TWO DIFFERENT REFERENCE SITES

In comparing the daytime attribution results with two different references sites, we find that the attributions resemble each other qualitatively except contributions from the aerodynamic resistance. In particular, the sign of the aerodynamic resistance difference is the opposite. Relative to the aerodynamic resistance of the urban site, the aerodynamic resistance of the short grassland site is much larger while that of the tall grassland site is slightly lower (Fig. 4e and Table 3).

We further find that the aerodynamic resistance difference is not entirely caused by the mean wind speed difference. The mean wind speed of the urban site is on average 0.5 and $0.3\,m\,s^{-1}$ higher than its counterparts at the tall and short grassland sites, respectively, during the daytime (Fig. 7). However, the aerodynamic resistance of the urban site is not always lower than that of the grassland sites. At the tall grassland site, although the mean wind is weaker compared to that at the urban site, the aerodynamic resistance is actually lower. In contrast, the short grassland site experiences lower mean wind speed, contributing to a larger aerodynamic resistance. These results suggest that the mean wind speed is not the only factor controlling the aerodynamic resistance and highlight that heat transfer is fundamentally different from momentum transfer over rough surfaces. We again stress that throughout the paper the aerodynamic resistance indicates the efficiency for convective heat transfer, not momentum transfer.

Similar to the daytime results, the fundamental difference between the two reference sites again lies in the contributions made by the aerodynamic resistance during nighttime. The aerodynamic resistance makes negative contribution for one reference site, the short grassland site, but positive contribution for another reference site, the tall grassland site (Tables 1 and 3). Also, the absolute values of the sensitivity and the difference when the tall grassland site is the reference site are smaller than those when the short grassland site is the reference site, causing a much smaller contribution from the aerodynamic resistance (in terms of absolute value) when using the tall grassland site as a reference.

There are two other minor differences that are worth mentioning. First, the contribution of the surface resistance when the tall grassland site is the reference site is smaller than its

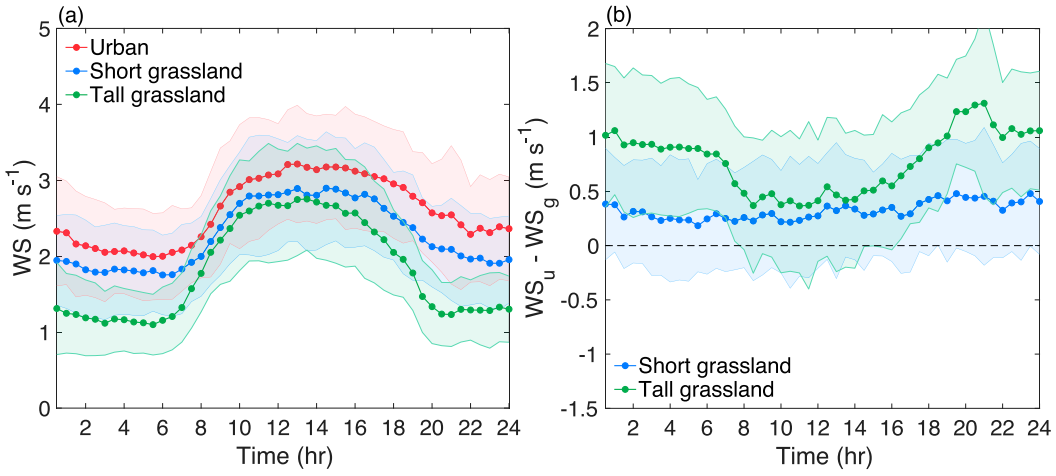

FIG. 7. Average diurnal cycles of (a) wind speeds and (b) differences in wind speed between the urban site and the grassland sites (urban minus grassland). The shading denotes standard deviations.

counterpart when the short grassland site is the reference site for both daytime and nighttime. This is mainly associated with the lower sensitivity of surface temperature to surface resistance at the tall grassland site, which is about 50% of its counterpart at the short grassland site (Table 2). Second, the contribution of air temperature when the tall grassland site is the reference is larger than that when the short grassland site is the reference site for both daytime and nighttime. This is because both the sensitivity and difference for the air temperature at the tall grassland site are about 2–3 times those at the short grassland site (Tables 2 and 3). While the overall effects of these differences on the attribution results are small, these differences highlight that a change in the reference site can cause both the surface temperature sensitivity and the urban–rural difference to change significantly.

4. Conclusions and discussions

In this study, we investigate the controlling factors of the SUHIs or SUCIs using pair flux tower data collected in and near the city of Nanjing, China. Two rural reference sites are used: one is over a tall grassland distant from the urban site and the other is over a short grassland relatively closer to the urban site. During the daytime, we identify a strong SUCI when the short grassland site is used as the reference site but a moderate SUHI when the tall grassland site is used as the reference site. The former is mainly caused by the larger aerodynamic resistance for convective heat transfer of the short grassland site than that of the urban site, while the latter is primarily attributed to the lower surface resistance of the tall grassland site than that of the urban site. At night, we find SUHIs when either of the grassland sites is used as the reference site, which are predominantly caused by the larger heat storage release at the urban site. Overall, the contributions of urban–rural differences in atmospheric conditions to the SUHIs or SUCIs are minor relative to those of surface biophysical properties but are nonnegligible especially for incoming shortwave and longwave radiation and air temperature.

One immediate implication of these findings is that the magnitude of SUHI can vary strongly with the characteristics of the rural land. Even with the same rural land-cover type (e.g., grassland), one could obtain either SUHI or SUCI depending on the grass height, and the associated physical drivers of urban–rural surface temperature difference are very different. This poses enormous challenges for applying knowledge obtained from single-point measurements to understanding large-scale observations such as remote sensing or large-scale simulations from global models.

Now let us return to the debate mentioned in the introduction that motivated our study. If we view the difference in the computed SUHIs when the rural reference site is switched as a manifestation of the spatial variability of SUHIs, then at first glance it appears that our findings support the conclusion of Zhao et al. (2014), that is, the spatial variations of daytime SUHIs are largely explained by the spatial variations of urban–rural differences in the aerodynamic resistance for convective heat transfer, which are further driven by the spatial variations of aerodynamic resistance of the rural land. Specifically, if the rural site has short and more sparse vegetation, it tends to have a large aerodynamic resistance, which leads to a low sensible heat flux and thus a high surface temperature. On the other hand, if the rural site has tall vegetation, it tends to have a small aerodynamic resistance, which leads to a high sensible heat flux and thus a low surface temperature.

However, this does not come without caveats. The most important caveat is the scale issue (Li and Wang 2019). The spatial variations of SUHIs in this study are intraurban variations within a metropolitan area while the original debate is about city-to-city variations across a continent. Another caveat is the methodological difference. The contrasting conclusions drawn from the previous two studies are also related to the difference in their attribution methods. Li et al. (2019) used the TRM method, which is similar to our study but did not consider urban–rural differences in atmospheric conditions (they did not need to because when using the subgrid-scale outputs there were no urban–rural differences in atmospheric conditions).

On the other hand, Zhao et al. (2014) used the so-called intrinsic biophysical mechanism (IBM) method, which used the Bowen ratio, or the ratio of sensible to latent heat fluxes, to replace the surface resistance in the attribution. In doing so, the IBM method assumed independence between the Bowen ratio and the aerodynamic resistance, just like the TRM method assumed independence between the surface resistance and the aerodynamic resistance. Later studies discovered that by assuming independence between the Bowen ratio and aerodynamic resistance, the contribution of aerodynamic resistance tends to be overestimated (Liao et al. 2018; Rigden and Li 2017) and the dominant control of spatial variations of SUHIs may be changed (Li et al. 2019). Here we only used the TRM method whose assumption is more justified at least from the perspective of land surface modeling.

Last, we comment on the role of ground heat flux or heat storage. While our finding that the larger heat storage release over urban areas at night is the main cause of nighttime SUHIs is consistent with the traditional paradigm (Oke et al. 2017), we have to acknowledge that the ground heat flux in our study actually reflects the combined effects of ''true'' ground heat flux, anthropogenic heat flux, advective heat flux, surface energy imbalance issues, and measurement errors. The available data do not allow us to separate these different players. Among them, however, only the true ground heat flux is expected to play opposite roles between day and night, namely, leaving the control volume during daytime and returning to the control volume during nighttime. There is no a priori reason to expect the other fluxes to behave in this manner. Thus, the observed opposite roles of ground heat flux during daytime and nighttime indicate that the true ground heat flux probably dominates over the other players.

Acknowledgments. Authors L. Wang and D. Li acknowledge support from the U.S. Army Research Office (Grant W911NF-18-1-0360) and the U.S. National Science Foundation (Grant ICER-1854706). Authors N. Zhang, J. Sun, and W. Guo acknowledge support from the Chinese National Key Research and Development Program (Grant 2016YFA0600303) and the National Natural Science Foundation of China (Grant 41675008).

REFERENCES

Aida, M., and M. Yaji, 1979: Observations of atmospheric downward radiation in the Tokyo area. *Bound.-Layer Meteor.*, **16**, 453–465, https://doi.org/10.1007/BF03335384.

Ao, X., L. Wang, X. Zhi, W. Gu, H. Yang, and D. Li, 2019: Observed synergies between urban heat islands and heat waves and their controlling factors in Shanghai, China. *J. Appl. Meteor. Climatol.*, **58**, 1955–1972, https://doi.org/10.1175/JAMC-D-19-0073.1.

Arnfield, A. J., 2003: Two decades of urban climate research: A review of turbulence, exchanges of energy and water, and the urban heat island. *Int. J. Climatol.*, **23**, 1–26, https://doi.org/10.1002/joc.859.

Brutsaert, W., 1982: *Evaporation into the Atmosphere: Theory, History and Applications*. Springer Netherlands, 302 pp.

——, 2005: *Hydrology: An Introduction*. Cambridge University Press, 605 pp.

Burakowski, E., A. Tawfik, A. Ouimette, L. Lepine, K. Novick, S. Ollinger, C. Zarzycki, and G. Bonan, 2018: The role of surface roughness, albedo, and Bowen ratio on ecosystem energy balance in the eastern United States. *Agric. For. Meteor.*, **249**, 367–376, https://doi.org/10.1016/j.agrformet.2017.11.030.

Carlson, T. N., and F. E. Boland, 1978: Analysis of urban–rural canopy using a surface heat flux/temperature model. *J. Appl. Meteor.*, **17**, 998–1013, https://doi.org/10.1175/1520-0450(1978)017<0998:AOURCU>2.0.CO;2.

Chen, C., Wang, L., Ranga, M., Li, D., 2020: Attribution of land-use/land-cover change induced surface temperature anomaly: How accurate is the first-order Taylor series expansion? *J. Geophys. Res. Biogeosci.*, **125**, e2020JG005787, https://doi.org/10.1029/2020JG005787.

Chen, L., and P. A. Dirmeyer, 2016: Adapting observationally based metrics of biogeophysical feedbacks from land cover/land use change to climate modeling. *Environ. Res. Lett.*, **11**, 034002, https://doi.org/10.1088/1748-9326/11/3/034002.

Christen, A., and R. Vogt, 2004: Energy and radiation balance of a central European city. *Int. J. Climatol.*, **24**, 1395–1421, https://doi.org/10.1002/joc.1074.

Cleugh, H. A., and T. R. Oke, 1986: Suburban–rural energy balance comparisons in summer for Vancouver, B.C. *Bound.-Layer Meteor.*, **36**, 351–369, https://doi.org/10.1007/BF00118337.

Estournel, C., R. Vehil, D. Guedalia, J. Fontan, and A. Druilhet, 1983: Observations and modeling of downward radiative fluxes (solar and infrared) in urban/rural areas. *J. Climate Appl. Meteor.*, **22**, 134–142, https://doi.org/10.1175/1520-0450(1983)022<0134:OAMODR>2.0.CO;2.

Foken, T., 2008: The energy balance closure problem: An overview. *Ecol. Appl.*, **18**, 1351–1367, https://doi.org/10.1890/06-0922.1.

Franssen, H. J. H., R. Stöckli, I. Lehner, E. Rotenberg, and S. I. Seneviratne, 2010: Energy balance closure of eddy-covariance data: A multisite analysis for European FLUXNET stations. *Agric. For. Meteor.*, **150**, 1553–1567, https://doi.org/10.1016/j.agrformet.2010.08.005.

Gan, C.-M., J. Pleim, R. Mathur, C. Hogrefe, C. N. Long, J. Xing, S. Roselle, and C. Wei, 2014: Assessment of the effect of air pollution controls on trends in shortwave radiation over the United States from 1995 through 2010 from multiple observation networks. *Atmos. Chem. Phys.*, **14**, 1701–1715, https://doi.org/10.5194/acp-14-1701-2014.

Garratt, J. R., 1992: *The Atmospheric Boundary Layer*. Cambridge University Press, 316 pp.

Grimm, N. B., S. H. Faeth, N. E. Golubiewski, C. L. Redman, J. Wu, X. Bai, and J. M. Briggs, 2008: Global change and the ecology of cities. *Science*, **319**, 756–760, https://doi.org/10.1126/science.1150195.

Grimmond, C. S. B., 2007: Urbanization and global environmental change: Local effects of urban warming. *Geogr. J.*, **173**, 83–88, https://doi.org/10.1111/j.1475-4959.2007.232_3.x.

——, and T. R. Oke, 1995: Comparison of heat fluxes from summertime observations in the suburbs of four North American cities. *J. Appl. Meteor.*, **34**, 873–889, https://doi.org/10.1175/1520-0450(1995)034<0873:COHFFS>2.0.CO;2.

——, J. A. Salmond, T. R. Oke, B. Offerle, and A. Lemonsu, 2004: Flux and turbulence measurements at a densely built-up site in Marseille: Heat, mass (water and carbon dioxide), and momentum. *J. Geophys. Res.*, **109**, D24101, https://doi.org/10.1029/2004JD004936.

Gu, Y., and D. Li, 2018: A modeling study of the sensitivity of urban heat islands to precipitation at climate scales. *Urban Climate*, **24**, 982–993, https://doi.org/10.1016/j.uclim.2017.12.001.

Guo, W., X. Wang, J. Sun, A. Ding, and J. Zou, 2016: Comparison of land–atmosphere interaction at different surface types in the mid- to lower reaches of the Yangtze River valley. *Atmos. Chem. Phys.*, **16**, 9875–9890, https://doi.org/10.5194/acp-16-9875-2016.

Imhoff, M. L., P. Zhang, R. E. Wolfe, and L. Bounoua, 2010: Remote sensing of the urban heat island effect across biomes in the continental USA. *Remote Sens. Environ.*, **114**, 504–513, https://doi.org/10.1016/j.rse.2009.10.008.

Jáuregui, E., and E. Luyando, 1999: Global radiation attenuation by air pollution and its effects on the thermal climate in Mexico City. *Int. J. Climatol.*, **19**, 683–694, https://doi.org/10.1002/(SICI)1097-0088(199905)19:6<683::AID-JOC389>3.0.CO;2-8.

Kalanda, B., T. Oke, and D. Spittlehouse, 1980: Suburban energy balance estimates for Vancouver, B.C., using the Bowen ratio-energy balance approach. *J. Appl. Meteor.*, **19**, 791–802, https://doi.org/10.1175/1520-0450(1980)019<0791:SEBEFV>2.0.CO;2.

Lee, X., and Coauthors, 2011: Observed increase in local cooling effect of deforestation at higher latitudes. *Nature*, **479**, 384–387, https://doi.org/10.1038/nature10588.

Leuning, R., E. van Gorsela, W. J. Massman, and P. R. Isaac, 2012: Reflections on the surface energy imbalance problem. *Agric. For. Meteor.*, **156**, 65–74, https://doi.org/10.1016/j.agrformet.2011.12.002.

Li, D., 2019: Turbulent Prandtl number in the atmospheric boundary layer – where are we now? *Atmos. Res.*, **216**, 86–105, https://doi.org/10.1016/j.atmosres.2018.09.015.

——, and L. Wang, 2019: Sensitivity of surface temperature to land use and land cover change-induced biophysical changes: The scale issue. *Geophys. Res. Lett.*, **46**, 9678–9689, https://doi.org/10.1029/2019GL084861.

——, T. Sun, M. Liu, L. Yang, L. Wang, and Z. Gao, 2015: Contrasting responses of urban and rural surface energy budgets to heat waves explain synergies between urban heat islands and heat waves. *Environ. Res. Lett.*, **10**, 054009, https://doi.org/10.1088/1748-9326/10/5/054009.

——, S. Malyshev, and E. Shevliakova, 2016a: Exploring historical and future urban climate in the Earth system modeling framework: 1. Model development and evaluation. *J. Adv. Model. Earth Syst.*, **8**, 917–935, https://doi.org/10.1002/2015MS000578.

——, ——, and ——, 2016b: Exploring historical and future urban climate in the Earth system modeling framework: 2. Impact of urban land use over the continental United States. *J. Adv. Model. Earth Syst.*, **8**, 936–953, https://doi.org/10.1002/2015MS000579.

——, W. Liao, A. J. Rigden, X. Liu, D. Wang, S. Malyshev, and E. Shevliakova, 2019: Urban heat island: Aerodynamics or imperviousness? *Sci. Adv.*, **5**, eaau4299, https://doi.org/10.1126/sciadv.aau4299.

Li, Q., and E. Bou-Zeid, 2019: Contrasts between momentum and scalar transport over very rough surfaces. *J. Fluid Mech.*, **880**, 32–58, https://doi.org/10.1017/jfm.2019.687.

——, ——, S. Grimmond, S. Zilitinkevich, and G. Katul, 2020: Revisiting the relation between momentum and scalar roughness lengths of urban surfaces. *Quart. J. Roy. Meteor. Soc.*, **146**, 3144–3164, https://doi.org/10.1002/qj.3839.

Liao, W., A. J. Rigden, and D. Li, 2018: Attribution of local temperature response to deforestation. *J. Geophys. Res. Biogeosci.*, **123**, 1572–1587, https://doi.org/10.1029/2018JG004401.

Liu, S. M., Z. W. Xu, W. Z. Wang, Z. Z. Jia, M. J. Zhu, J. Bai, and J. M. Wang, 2011: A comparison of eddy-covariance and large aperture scintillometer measurements with respect to the energy balance closure problem. *Hydrol. Earth Syst. Sci.*, **15**, 1291–1306, https://doi.org/10.5194/hess-15-1291-2011.

Manoli, G., and Coauthors, 2019: Magnitude of urban heat islands largely explained by climate and population. *Nature*, **573**, 55–60, https://doi.org/10.1038/s41586-019-1512-9.

Mauder, M., M. Cuntz, C. Drüe, A. Graf, C. Rebmann, H. P. Schmid, M. Schmidt, and R. Steinbrecher, 2013: A strategy for quality and uncertainty assessment of long-term eddy-covariance measurements. *Agric. For. Meteor.*, **169**, 122–135, https://doi.org/10.1016/j.agrformet.2012.09.006.

Monteith, J., and M. Unsworth, 2007: *Principles of Environmental Physics*. Academic Press, 440 pp.

Moon, M., D. Li, W. Liao, A. J. Rigden, and M. A. Friedl, 2020: Modification of surface energy balance during springtime: The relative importance of biophysical and meteorological changes. *Agric. For. Meteor.*, **284**, 107905, https://doi.org/10.1016/j.agrformet.2020.107905.

Mora, C., and Coauthors, 2017: Global risk of deadly heat. *Nat. Climate Change*, **7**, 501–506, https://doi.org/10.1038/nclimate3322.

Núñez, M., I. Eliasson, and J. Lindgren, 2000: Spatial variation of incoming longwave radiation in Göteborg, Sweden. *Theor. Appl. Climatol.*, **67**, 181–192, https://doi.org/10.1007/s007040070007.

Offerle, B., C. S. B. Grimmond, K. Fortuniak, K. Kłysik, and T. R. Oke, 2006: Temporal variations in heat fluxes over a central European city centre. *Theor. Appl. Climatol.*, **84**, 103–115, https://doi.org/10.1007/s00704-005-0148-x.

Oke, T. R., 1982: The energetic basis of the urban heat island. *Quart. J. Roy. Meteor. Soc.*, **108**, 1–24, https://doi.org/10.1002/qj.49710845502.

——, 1988: The urban energy balance. *Prog. Phys. Geogr.*, **12**, 471–508, https://doi.org/10.1177/030913338801200401.

——, and R. F. Fuggle, 1972: Comparison of urban/rural counter and net radiation at night. *Bound.-Layer Meteor.*, **2**, 290–308, https://doi.org/10.1007/BF02184771.

——, G. Mills, A. Christen, and J. A. Voogt, 2017: *Urban Climate*. Cambridge University Press, 546 pp.

Oleson, K. W., G. B. Bonan, J. Feddema, and M. Vertenstein, 2008a: An urban parameterization for a global climate model. Part II: Sensitivity to input parameters and the simulated urban heat island in offline simulations. *J. Appl. Meteor. Climatol.*, **47**, 1061–1076, https://doi.org/10.1175/2007JAMC1598.1.

——, ——, ——, ——, and C. S. B. Grimmond, 2008b: An urban parameterization for a global climate model. Part I: Formulation and evaluation for two cities. *J. Appl. Meteor. Climatol.*, **47**, 1038–1060, https://doi.org/10.1175/2007JAMC1597.1.

Peng, S., and Coauthors, 2012: Surface urban heat island across 419 global big cities. *Environ. Sci. Technol.*, **46**, 696–703, https://doi.org/10.1021/es2030438.

Peterson, J., and E. Flowers, 1977: Interactions between air-pollution and solar-radiation. *Sol. Energy*, **19**, 23–32, https://doi.org/10.1016/0038-092X(77)90085-8.

Ramamurthy, P., E. Bou-Zeid, J. A. Smith, Z. Wang, M. L. Baeck, N. Z. Saliendra, J. L. Hom, and C. Welty, 2014: Influence of subfacet heterogeneity and material properties on the urban surface energy budget. *J. Appl. Meteor. Climatol.*, **53**, 2114–2129, https://doi.org/10.1175/JAMC-D-13-0286.1.

Rigden, A. J., and D. Li, 2017: Attribution of surface temperature anomalies induced by land use and land cover changes. *Geophys. Res. Lett.*, **44**, 6814–6822, https://doi.org/10.1002/2017GL073811.

Rydin, Y., and Coauthors, 2012: Shaping cities for health: Complexity and the planning of urban environments in the 21st century. *Lancet*, **379**, 2079–2108, https://doi.org/10.1016/S0140-6736(12)60435-8.

Stanhill, G., and S. Moreshet, 1994: Global radiation climate change at seven sites remote from surface sources of pollution. *Climatic Change*, **26**, 89–103, https://doi.org/10.1007/BF01094010.

Stoy, P. C., and Coauthors, 2013: A data-driven analysis of energy balance closure across FLUXNET research sites: The role of landscape scale heterogeneity. *Agric. For. Meteor.*, **171–172**, 137–152, https://doi.org/10.1016/j.agrformet.2012.11.004.

Taha, H., 1997: Urban climates and heat islands: Albedo, evapotranspiration, and anthropogenic heat. *Energy Build.*, **25**, 99–103, https://doi.org/10.1016/S0378-7788(96)00999-1.

United Nations, 2019: *World Urbanization Prospects: The 2018 Revision*. United Nations, 103 pp.

Wang, L., Z. Gao, S. Miao, X. Guo, T. Sun, M. Liu, and D. Li, 2015: Contrasting characteristics of the surface energy balance between the urban and rural areas of Beijing. *Adv. Atmos. Sci.*, **32**, 505–514, https://doi.org/10.1007/s00376-014-3222-4.

Wang, P., D. Li, W. Liao, A. Rigden, and W. Wang, 2019: Contrasting evaporative responses of ecosystems to heatwaves traced to the opposing roles of vapor pressure deficit and surface resistance. *Water Resour. Res.*, **55**, 4550–4563, https://doi.org/10.1029/2019WR024771.

Wang, X., W. Guo, B. Qiu, Y. Liu, J. Sun, and A. Ding, 2017: Quantifying the contribution of land use change to surface temperature in the lower reaches of the Yangtze River. *Atmos. Chem. Phys.*, **17**, 4989–4996, https://doi.org/10.5194/acp-17-4989-2017.

Yap, D., and T. R. Oke, 1974: Sensible heat fluxes over an urban area—Vancouver, B.C. *J. Appl. Meteor.*, **13**, 880–890, https://doi.org/10.1175/1520-0450(1974)013<0880:SHFOAU>2.0.CO;2.

Zhao, L., X. Lee, R. B. Smith, and K. Oleson, 2014: Strong contributions of local background climate to urban heat islands. *Nature*, **511**, 216–219, https://doi.org/10.1038/nature13462.

——, M. Oppenheimer, Q. Zhu, J. W. Baldwin, K. L. Ebi, E. Bou-Zeid, K. Guan, and X. Liu, 2018: Interactions between urban heat islands and heat waves. *Environ. Res. Lett.*, **13**, 034003, https://doi.org/10.1088/1748-9326/aa9f73.

Zhou, D., L. Zhang, D. Li, D. Huang, and C. Zhu, 2016: Climate–vegetation control on the diurnal and seasonal variations of surface urban heat islands in China. *Environ. Res. Lett.*, **11**, 074009, https://doi.org/10.1088/1748-9326/11/7/074009.